

*The rate of viral transfer between upper and lower respiratory tracts determines RSV illness duration*

**Gilberto González-Parra & Hana M. Dobrovolny**

**Journal of Mathematical Biology**

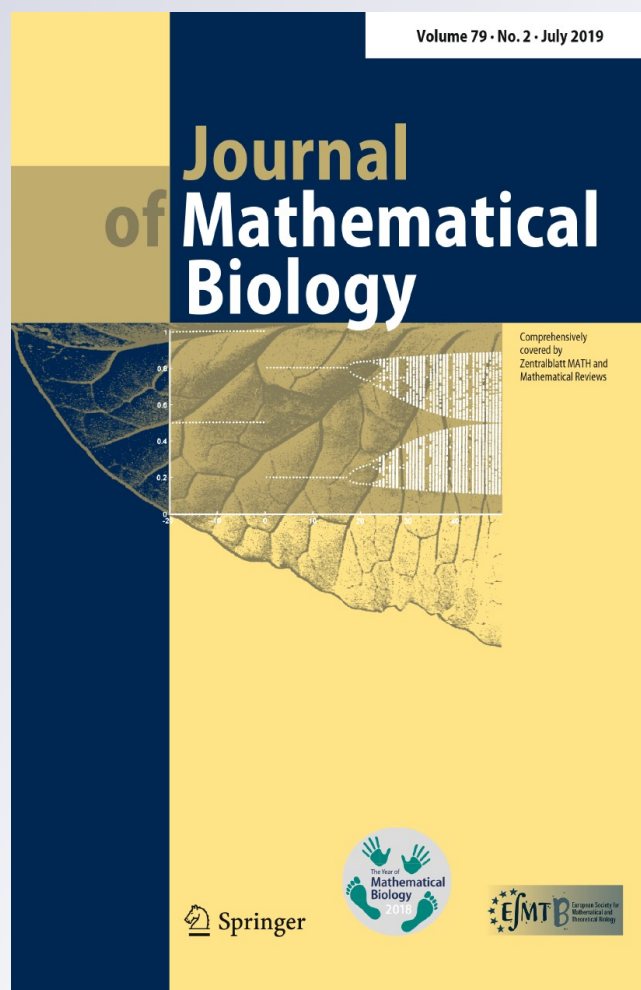
ISSN 0303-6812

Volume 79

Number 2

J. Math. Biol. (2019) 79:467–483


DOI 10.1007/s00285-019-01364-1



**Your article is protected by copyright and all rights are held exclusively by Springer-Verlag GmbH Germany, part of Springer Nature. This e-offprint is for personal use only and shall not be self-archived in electronic repositories. If you wish to self-archive your article, please use the accepted manuscript version for posting on your own website. You may further deposit the accepted manuscript version in any repository, provided it is only made publicly available 12 months after official publication or later and provided acknowledgement is given to the original source of publication and a link is inserted to the published article on Springer's website. The link must be accompanied by the following text: "The final publication is available at [link.springer.com](http://link.springer.com)".**



# The rate of viral transfer between upper and lower respiratory tracts determines RSV illness duration

Gilberto González-Parra<sup>1,2</sup> · Hana M. Dobrovolny<sup>1</sup> 

Received: 5 February 2018 / Revised: 11 April 2019 / Published online: 22 April 2019  
© Springer-Verlag GmbH Germany, part of Springer Nature 2019

## Abstract

Respiratory syncytial virus can lead to serious lower respiratory infection (LRI), particularly in children and the elderly. LRI can cause longer infections, lingering respiratory problems, and higher incidence of hospitalization. In this paper, we use a simplified ordinary differential equation model of viral dynamics to study the role of transport mechanisms in the occurrence of LRI. Our model uses two compartments to simulate the upper respiratory tract and the lower respiratory tract (LRT) and assumes two distinct types of viral transfer between the two compartments: diffusion and advection. We find that a range of diffusion and advection values lead to long-lasting infections in the LRT, elucidating a possible mechanism for the severe LRI infections observed in humans.

**Keywords** Respiratory syncytial virus · Mathematical model · Diffusion · Advection · Lower respiratory infection

**Mathematics Subject Classification** 92C99

## 1 Introduction

The disease burden from respiratory syncytial virus (RSV) can be substantial, causing death and hospitalization in infants (Geoghegan et al. 2017) and the elderly (Fleming

---

**Electronic supplementary material** The online version of this article (<https://doi.org/10.1007/s00285-019-01364-1>) contains supplementary material, which is available to authorized users.

---

✉ Hana M. Dobrovolny  
h.dobrovolny@tcu.edu  
Gilberto González-Parra  
gilberto.gonzalezparra@nmt.edu

<sup>1</sup> Texas Christian University, Fort Worth, TX, USA

<sup>2</sup> Present Address: New Mexico Tech, Socorro, NM, USA

et al. 2015). However, RSV causes only mild infections in healthy adults (Hall et al. 2001; Lee et al. 2004; Bagga et al. 2013; Mills et al. 1971). One possible reason for some of the difference in disease severity is the more frequent involvement of the lower respiratory tract (LRT) during infections in infants and the elderly (Naorat et al. 2013; Kaneko et al. 2001; Shi et al. 2015; Atwell et al. 2016; Hall et al. 2001; Takeyama et al. 2016; Park et al. 2017).

In fact, RSV is the most common cause of acute lower respiratory infection (LRI) in small children (Nair et al. 2010; Forster et al. 2004) and leads to long-term changes in lung function (Hosakote et al. 2016; Guerrero-Plata et al. 2009; Mejias et al. 2008; Zeng et al. 2011) which leads to lingering respiratory problems (Poulsen et al. 2006; Fauroux et al. 2017; Palmer et al. 2010; Backman et al. 2014). Specifically, studies have found increased wheezing in children who have experienced RSV-induced LRI (Bont et al. 2004; Fauroux et al. 2017) lasting up to 5 years. More worryingly, there appears to be an increase in cases of asthma among children who have had RSV-induced LRI (Piedimonte 2013; Perez-Yarza et al. 2007; Zeng et al. 2011). LRI in older adults is linked to a higher incidence of life-threatening infections requiring ventilation and ICU admission (Park et al. 2017; Branche and Falsey 2015; Lee et al. 2015). It also causes serious illness and death in immunocompromised adults (Robert et al. 2008; Ebbert and Limper 2005).

Studies have found that there are differences in spread of RSV infection between the upper respiratory tract (URT) and the lower respiratory tract (Kim et al. 2016; Grieves et al. 2015; Walpita et al. 2015). One possible cause of these differences is different immune responses in the URT and LRT (Everard et al. 1994; Plotnicky-Gilquin et al. 2000; Sealy et al. 2017). However, there also appear to be fundamental differences in virus-cell interactions in cells taken from the URT and the LRT (Guo-Parke et al. 2013; Spann et al. 2014) that can also lead to altered disease spread in the URT and LRT. A better understanding of how the disease spreads within each part of the respiratory tract and how it spreads from URT to LRT could help prevent more severe disease.

Mathematical modeling is one technique that can help develop a better understanding of some of the biological processes that contribute to dynamics of viral infections. While spatial spread of infections is sometimes studied using computationally expensive agent-based models (Goyal and Murray 2016; Beauchemin et al. 2005; dos Santos and Coutinho 2001; Strain et al. 2002; Gallagher et al. 2018), insight into mechanisms of viral spread can also be gleaned from simpler differential equation models (Allen and Schwartz 2015; Wang et al. 2017; Frank 2000; Reperant et al. 2012). Unfortunately, these models rarely examine the role of viral transport mechanisms. There are two viral transport mechanisms in the respiratory tract, diffusion and advection. Diffusion moves virus from regions of high concentration to regions of low concentration. Advection is caused by the mucociliary escalator that moves at roughly constant velocity and can sweep virions towards the top of the respiratory tract (Murphy and Florman 1983). Some mathematical models have explored the role of diffusion in the spread of influenza virus (Bocharov et al. 2016; Holder et al. 2011a,b) finding that the rate of diffusion plays a role in formation of plaques in vitro (Holder et al. 2011a), determines how quickly plaques grow (Holder et al. 2011b), and determines the stability of traveling waves of infection (Bocharov et al. 2016). While diffusion is the dominant transport process in vitro, advection within mucociliary flow also transports

viruses in the respiratory tract (Kesimer et al. 2013). Mucociliary flow drives inhaled virus particles upward (Anekal et al. 2009), helping to prevent spread to the LRT (Vareille et al. 2011). It is not yet clear how the two transport mechanisms interact to either allow or prevent LRI.

In this paper, we propose a differential equation model for RSV that tracks viral dynamics in both the URT and the LRT. In the model, virus travels between the URT and LRT via two mechanisms: diffusion allows the virus to travel in either direction, and advection, upward motion of virus driven by the mucociliary escalator, drives virus from the LRT to the URT. We fit the model to data from RSV infections in ferrets, finding that advection is the stronger transport mechanism in these animals. We then fit the model to data from pediatric patients to estimate the probability that the LRT is involved in the infection.

## 2 Methods

### 2.1 Mathematical model

We propose a two-compartment model based on the viral kinetics model presented in Baccam et al. (2006). While the model in Baccam et al. (2006) was proposed for influenza, it is applicable to other respiratory viral infections including RSV (González-Parra and Dobrovoly 2018a) due to the similarity in infection dynamics. The model has two compartments, one representing the URT, the second representing the LRT. Within each compartment, infection dynamics are modeled with an exponential viral kinetics model. Virus can move between the two compartments by one of two methods: diffusion which moves virus from areas of higher concentration to areas of lower concentration, and advection which represents virus transport via the mucociliary escalator which moves virus upwards only. The model equations are as follows:

$$\begin{aligned}
 \text{Target cells:} \quad & \frac{dT_U}{dt} = -\beta_U T_U V_U & \frac{dT_L}{dt} &= -\beta_L T_L V_L \\
 \text{Eclipse cells:} \quad & \frac{dE_U}{dt} = \beta_U T_U V_U - k_U E_U & \frac{dE_L}{dt} &= \beta_L T_L V_L - k_L E_L \\
 \text{Infectious cells:} \quad & \frac{dI_U}{dt} = k_U E_U - \delta_U I_U & \frac{dI_L}{dt} &= k_L E_L - \delta_L I_L \\
 \text{Virus:} \quad & \frac{dV_U}{dt} = p_U I_U - D(V_U - V_L) & \frac{dV_L}{dt} &= p_L I_L + D(V_U - V_L) \\
 & - \nu V_U + \nu V_L & & - c_L V_L - \nu V_L
 \end{aligned} \tag{1}$$

The  $U$  subscript represents the URT while the  $L$  subscript represents the LRT. Within each compartment, target cells  $T_i$  (where  $i = U, L$ ) are infected by virus  $V_i$  at a rate  $\beta_i$ . Once infected, the cells enter an eclipse phase  $E_i$  where the cells are not actively producing virus. After an average time  $1/k_i$ , the cells start producing virus and enter the infectious phase  $I_i$ . They remain in this phase for an average time  $1/\delta_i$  and produce virions at a rate  $p_i$ . Virus is cleared at a rate  $c_i$ . The term  $D(V_U - V_L)$  represents viral movement through diffusion. If there is more virus in the URT than the LRT, virus will leave the URT and move to the LRT; while if there is more virus in the LRT, virus will

move in the other direction. The term  $\nu V_L$  represents upward movement of the virus through mucociliary clearance. An ODE model consisting of three respiratory tract compartments was previously proposed and analyzed (Reperant et al. 2012). However, that model did not consider specific transport mechanisms between the compartments.

We use a simplified model of infection within each compartment in order to minimize the number of free parameters and focus on transport mechanisms, but more realistic models are available. For example, transitions between the eclipse and infectious compartments are most likely not exponentially distributed (Kakizoe et al. 2015). Similarly, transitions between infectious dead cells are also likely not exponentially distributed (Beauchemin et al. 2017), and models using other distributions have been explored (Holder and Beauchemin 2011). The model also does not include an immune response, either innate or adaptive. While some of the effect of the immune response can be implicitly modeled by changing parameter values (a larger value of viral clearance can account for the effect of antibodies), more realistic viral dynamics models that include an immune response are available and can be considered (Dobrovolny et al. 2013; Cao and McCaw 2017; Yan et al. 2017). Implications of these simplifications are considered in the discussion.

## 2.2 Animal infection experiments

Data from infections in ferrets was collected from the literature (Prince and Porter 1976). Ferrets were infected intranasally with  $3.6 \times 10^3$  pfu of RSV. At intervals after infection, animals were sacrificed and lung and nasal tissues were separately homogenized. Virus in lungs and nasal tissues was measured by plaque assay in HEP-2 cells. Data was extracted from the original publications using WebPlotDigitizer (<https://automeris.io/WebPlotDigitizer/>).

## 2.3 Pediatric infection

Data from pediatric infections was provided by Janssen R&D Belgium. RSV was diagnosed upon presentation at a doctor or hospital with viral titer measurements and symptom scores taken daily from that point until resolution of the infection.

## 2.4 Fitting experimental data

We implemented a Bayesian approach via Markov Chain Monte Carlo (MCMC) to estimate parameters. Least-squares estimates were used as the initial estimates for our implementation of the Bayesian approach (Worden and Hensman 2012). The sum of squared residuals (SSR) in this case contains two parts. For the animal studies, virus in the URT was fit to nasal viral data while virus in the LRT was fit to lung viral data, with both parts included in the calculation of SSR. For the pediatric study, virus in the URT was fit to viral titer measurements while the virus in the LRT was scaled and fit to the symptom score. All the model parameters were assumed to have uniform prior distributions. Uniform prior distributions are commonly used when there is not avail-

able information for the priors (Parkinson et al. 2006). We use the Matlab `gwmcmc` function, which is an implementation of the Goodman and Weare affine invariant ensemble MCMC sampler (Goodman and Weare 2010), to implement MCMC estimation. This function requires that we initialize the ensemble of walkers in a small Gaussian ball around the initial guess. In our work, we decided to use a Gaussian-type likelihood function because it is the method of choice found in the literature and has desirable asymptotic properties (Stoffer and Wall 1991). Minimizing the proposed likelihood function minimizes the difference between the viral related data corresponding to both tracts and the prediction produced by our proposed diffusion model. Furthermore, under some conditions minimizing a Gaussian likelihood is equivalent to the least squares method. Posterior distributions were determined using 20 walkers, 10,000 samples, a burn-in of 1000 samples and thinning by taking every 10th sample.

For the fits, we assumed that the initial number of target cells in both compartments was one and that the infection was initiated with some initial amount of virus in the upper compartment (to be fit). The initial number of eclipse and infectious cells was assumed to be zero. Note that this assumption results in reporting of cells (in any compartment) as proportions, rather than total number of cells. We also assumed that parameters describing host-virus interactions ( $p$ ,  $\beta$ ,  $c$ ,  $k$ ,  $\delta$ ) were the same in both compartments. While this is an oversimplification, there is not enough data to identify all the parameters. Fits of the ferret data where we have relaxed this assumption and allowed  $\beta$  and  $p$  to differ between the URT and LRT are presented in the supplementary material.

### 3 Results

#### 3.1 The roles of advection and diffusion

In our initial investigation of the model, we assume that infection dynamics are the same in both compartments (i.e all the parameters have the same value) and examine the dynamics over a range of values for the diffusion and advection parameters ( $D$  and  $\nu$ ). The parameters used for this investigation are taken from Baccam et al. (2006) and describe in vivo influenza infection. Parameters are given in Table 1. We assume that there are  $4.0 \times 10^8$  cells in each compartment and that the infection starts in the URT with an initial viral inoculum of  $7.5 \times 10^{-2}$  TCID<sub>50</sub>/mL. We then explore how the infection changes as we vary diffusion and advection constants.

**Table 1** Parameters for general investigation of the two compartment model, taken from Baccam et al. (2006)

Parameter	Value
$\beta$	$3.2 \times 10^{-5}$ mL/TCID <sub>50</sub> day <sup>-1</sup>
$p$	$4.6 \times 10^{-2}$ TCID <sub>50</sub> /mL day <sup>-1</sup>
$k$	4.0/day
$\delta$	5.2/day
$c$	5.2/day

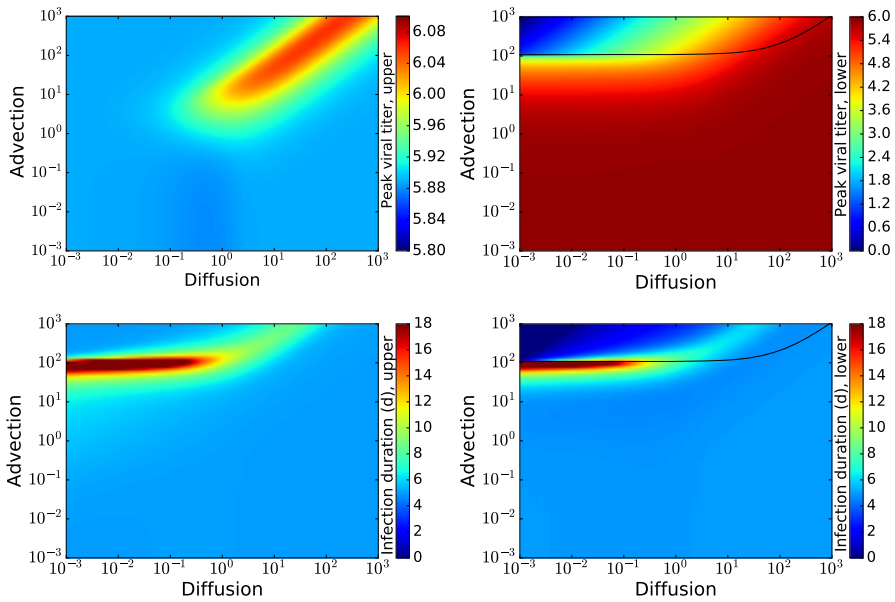


**Fig. 1** Effect of advection and diffusion in the two compartment model. The top row shows the peak viral titer in the upper compartment (left) and in the lower compartment (right). The bottom row shows the duration of the infection (time spent above  $10^1$  TCID<sub>50</sub>/mL) in the upper compartment (left) and in the lower compartment (right). The line indicates the boundary where  $R_{0L} = 1$ . Note that the colorbar scale on the upper left figure differs from the scale on the other three figures (color figure online)

In Fig. 1, we show the peak viral titer in the upper compartment (left) and in the lower compartment (right) in the top row and the duration of the infection in the upper compartment (left) and in the lower compartment (right) in the bottom row. When the advection is high and diffusion is low (top left corner of each plot), there is no infection in the lower compartment (peak titer and duration in the lower compartment go to zero). The advection is strong enough to clear away any virus that manages to diffuse down to the lower compartment. When advection is not quite strong enough to clear away the virus in the lower compartment, we see a small region of longer lasting infections (dark red region). In this region, diffusion is low, but advection is not quite strong enough to clear all the virus from the lower compartment, so there is a delay in spreading the infection from the upper compartment to the lower compartment. Once the infection has been initiated in the lower compartment, the strong advection sweeps much of the virus to the upper compartment, slowing growth of the infection in the lower compartment, but also preventing the decline of virus in the upper compartment.

This is shown more clearly in Fig. 2 where we show viral time courses for fixed diffusion and three different values of advection. The left-most graph shows the viral load in the URT (black line) and the LRT (red line) in the case of low advection. The infection starts in the URT and virus diffuses to the LRT where it starts another infection with some time delay. Virus from the infection in the LRT is moved back up to the URT, causing a second peak in the URT viral titer. Both infections clear when target cells are consumed in both compartments. The central graph shows the viral



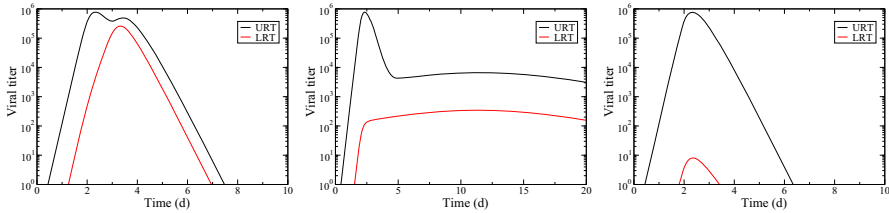


**Fig. 2** Effect of advection on viral kinetics. The diffusion parameter was fixed to  $D = 10^{-2}$ /day. Low advection ( $v = 10$ /day) causes a delayed infection in the LRT which pushes extra virus into the URT causing a secondary viral peak (left). Slightly higher advection ( $v = 100$ /day) causes a slow-growing infection in the LRT with viral levels remaining high in the URT because virus is moved upwards (center). High advection ( $v = 1000$ /day) prevents wide-spread infection of the LRT since any virus in the LRT is quickly moved up to the URT

load in the case of advection in the “long-lasting” zone. In this case, advection is strong enough to move lots of virus from the LRT to the URT, but not quite strong enough to prevent infection. The infection consumes the cells in the LRT slowly, leading to a long-lasting infection in the LRT. Since advection is strong, viral load in the URT also remains high, not because of continuing infection in the URT, but because virus is swept up from the LRT. The right-most graph shows the viral titer in the case of high advection. Here the advection is strong enough to remove any virus from the LRT before it can take hold and cause an infection.

We can determine the boundary for spread of the infection into the LRT by examining the basic reproductive number for this model which is given by

$$R_0 = \frac{D(D + v)}{(D + c_U)(D + c_L + v)} + \frac{p_L \beta_L T_L}{\delta_L (D + c_L + v)} + \frac{p_U \beta_U T_U}{\delta_U (D + c_U)} - \frac{p_L p_U \beta_L \beta_U T_L T_U}{\delta_L \delta_U (D + c_L + v)(D + c_U)} \tag{2}$$

The first term of this equation represents the ratio of flow of virus into the two compartments to the flow of virus out of the two compartments. The second term is the basic reproductive number of the LRT and the third term is the basic reproductive number of the URT. When the basic reproductive number is greater than 1, the infection spreads, but if  $R_0$  is less than one, the infection is suppressed. Note that this is the basic reproductive number for the full model, but if we want to know whether the infection will spread in the LRT, we need to consider the basic reproductive number for the LRT only,

$$R_{0L} = \frac{p_L \beta_L T_L}{\delta_L (D + c_L + v)}. \tag{3}$$

Growth of the infection in the LRT will occur if  $R_{0L} > 1$ , so the boundary is given by

$$v = \frac{p_L \beta_L T_L}{\delta_L} - D - c_L \tag{4}$$

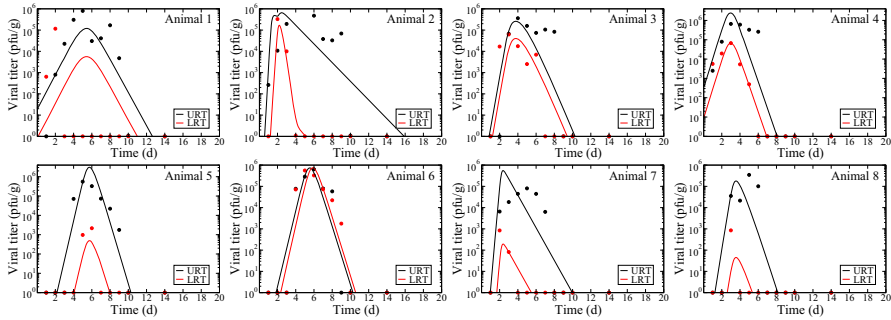


**Fig. 3** Fits of the model to RSV infections in ferrets. Black squares indicate viral titers measured from nasal samples while red squares indicate virus measured in the lungs. Black and red lines show the model best fit curves for the URT and LRT, respectively (color figure online)

This boundary is shown in Fig. 1. Note that the region of long-lasting infections lies along this boundary when  $R_{0L}$  is slightly greater than 1.

### 3.2 Animal infections

We fit the model to data from RSV infection of ferrets (Prince and Porter 1976). Experimental data and model fits are shown in Fig. 3 with the corresponding best fit parameters given in Table 2 and posterior distributions given in the supplementary material. The median clearance rate is similar to the RSV clearance rates found for humans (González-Parra and Dobrovolny 2015, 2018b) and African green monkeys (AGM) (González-Parra and Dobrovolny 2018a, b), while the eclipse duration ( $1/k$ ) and the infectious cell lifespan ( $1/\delta$ ) are both somewhat shorter than those found for humans and AGM (González-Parra and Dobrovolny 2015, 2018a, b). For most animals, the model fits the data reasonably well, although it has trouble fitting those animals for which viral peak in the URT and LRT do not occur at the same time. We find that in all but one case (Animal 6), the diffusion rate is slower than the advection rate, so there is net movement of the virus upwards. This is seen in low viral titers in the LRT.

### 3.3 Pediatric infections

Since pediatric patients are particularly susceptible to LRT infections from RSV (Nair et al. 2010; Forster et al. 2004), we also fit the model to data from RSV infections in pediatric patients. In this case, we did not have viral titer measurements from the LRT so we used the acute respiratory infection (ARI) symptom score as a proxy. The ARI assesses the severity of several respiratory symptoms. We assumed that the ARI score was proportional, with proportionality constant  $\alpha$ , to the log of the viral load in the LRT. The model fits are shown in Fig. 4 and the corresponding parameter estimates are shown in Table 3 with posterior distributions for all parameters included in the supplementary material. We see that the fit for one of the pediatric patients (Patient

**Table 2** Best fit parameters for model fits to RSV infections in ferrets

Parameter	$p$ (/h)	$\beta$ (/h)	$c$ (/h)	$1/\delta$ (h)	$1/k$ (h)
Animal 1	$4.0 \times 10^7$	$6.4 \times 10^{-8}$	0.61	0.28	0.51
Animal 2	$2.4 \times 10^5$	$1.0 \times 10^{-5}$	0.042	2.9	2.9
Animal 3	$9.0 \times 10^4$	$4.4 \times 10^{-6}$	0.12	8.1	9.3
Animal 4	$3.0 \times 10^7$	$1.9 \times 10^{-8}$	0.35	1.1	0.66
Animal 5	$5.5 \times 10^6$	$7.7 \times 10^{-8}$	0.17	2.3	4.5
Animal 6	$1.9 \times 10^8$	$1.6 \times 10^{-7}$	44	4.9	4.7
Animal 7	$4.1 \times 10^5$	$1.9 \times 10^{-6}$	0.074	2.2	1.2
Animal 8	$8.7 \times 10^4$	$1.9 \times 10^{-6}$	0.14	7.2	0.26
Median	$3.0 \times 10^6$	$1.0 \times 10^{-6}$	0.15	2.6	2.0
Parameter	$D$ (/h)	$\nu$ (/h)	$D/\nu$	$V_0$ (pfu/g)	SSR
Animal 1	0.11	2.3	0.048	29	46
Animal 2	$5.7 \times 10^{-6}$	0.31	$1.8 \times 10^{-5}$	$9.0 \times 10^{-5}$	21
Animal 3	0.29	2.0	0.15	0.030	35
Animal 4	0.49	18	0.028	550	15
Animal 5	0.0022	14	$1.5 \times 10^{-4}$	$9.2 \times 10^{-5}$	11
Animal 6	0.46	0.018	26	0.12	19
Animal 7	0.013	39	$3.3 \times 10^{-4}$	$3.5 \times 10^{-5}$	14
Animal 8	0.021	83	$2.5 \times 10^{-4}$	$1.0 \times 10^{-3}$	20
Median	0.067	8.2	0.014	0.016	20

Posterior distributions for all parameters are in the supplementary material

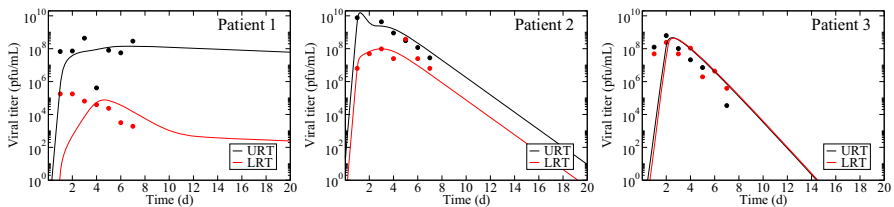


**Fig. 4** Fits of the model to RSV infections in pediatric patients. Black squares indicate viral titer measurements from patient nasal swabs. Red squares indicate the ARI score scaled by a factor of  $\alpha$ . Black and red lines indicate the model best fit curves for the URT and LRT, respectively (color figure online)

1) suggests that this patient is in the region where advection is not strong enough to fully clear virus from the LRT which leads to a long-lasting infection.

## 4 Discussion

In this paper, we describe a mathematical model that separately considers infection in the URT and LRT. While not a full spatiotemporal model of respiratory tract infection,

**Table 3** Best fit parameters for model fits to RSV infections in pediatric patients

Parameter	$p$ (/h)	$\beta$ (/h)	$t_{inf}$ (h)	$c$ (/h)	$1/\delta$ (h)	$1/k$ (h)
Patient 1	$6.5 \times 10^6$	$1.9 \times 10^{-6}$	0.40	0.0029	14	21
Patient 2	$1.2 \times 10^{11}$	$1.6 \times 10^{-10}$	0.32	3.2	6.2	4.8
Patient 3	$3.2 \times 10^{10}$	$3.7 \times 10^{-9}$	0.13	26	13	12
Parameter	$D$ (/h)	$\nu$ (/h)	$D/\nu$	$\alpha$	$V_0$ (pfu/g)	SSR
Patient 1	$8.1 \times 10^{-5}$	20	$4.0 \times 10^{-6}$	0.20	0.0079	0.76
Patient 2	0.12	78	0.0015	0.28	120	2.6
Patient 3	0.48	0.90	0.53	0.35	0.27	1.4

Posterior distributions for all parameters are included in the supplementary material

this simplified model allows examination of the roles of advection and diffusion in allowing spread of infections to the LRT. We found that this model predicts long-lasting viral infections in cases where the advection is not strong enough to fully prevent infection in the LRT by sweeping all virus out of the LRT. Advection cannot be so weak, however, that a homeostatic balance is maintained between virus in the LRT and URT. Note that we observe this change in viral kinetics without assuming that there are differences in the virus-host interactions in the LRT and URT.

There is evidence that mucus velocity is lower in small children (Sturm 2012; Puchelle et al. 1979) and that it decreases again in the elderly (Grubb et al. 2016; de Oliveira-Maul et al. 2013; Ho et al. 2001). These two populations are also the ones that are particularly susceptible to LRT (Naorat et al. 2013; Kaneko et al. 2001; Shi et al. 2015; Atwell et al. 2016; Hall et al. 2001; Takeyama et al. 2016; Park et al. 2017). Since diffusion rate is determined by particle size, temperature, and fluid viscosity (Cush et al. 1997), all of which do not vary with age, our model suggests that differences in susceptibility to LRT could be due to changes in the advection rate. The lowered advection rate in these two populations might land them in the region where virus is not only able to move down to the LRT to establish an infection, but once there, will cause a long-lasting infection. Other respiratory viruses also appear to be more likely to cause LRI in children and the elderly (Kusel et al. 2006; Wolf et al. 2006; GBD 2017), possibly due to the lowered advection rate of these two populations. Other causes of the increased susceptibility to LRI have also been examined. Some studies have cited differing immune response as a possible contributor to LRI (Zhao et al. 2017; Laham et al. 2004; Moore et al. 2013), suggesting that the weakened immune response in small children (Ruckwardt et al. 2016; Tregoning and Schwarze 2010) and in the elderly (Walsh et al. 2013) allows for viral spread to the LRT.

While our model is highly simplified, using only two compartments to represent spatial distribution, it does include two distinct transport mechanisms, allowing for evaluation of the role of each mechanism in the spread of virus. Partial differential equation (PDE) models would allow for more detailed examination of spatial spread of virus, perhaps pinpointing how far down the respiratory tract virus can spread as diffusion and advection are varied. While PDE models have previously been used to

study the spatial spread of virus (Bocharov et al. 2016; Holder et al. 2011a, b), they have so far only included diffusion as a transport mechanism. An additional simplification is the use of continuous ordinary differential equations to model an inherently stochastic system (Yan et al. 2016; Bai and Allen 2019). A stochastic implementation of the model would essentially blur the hard boundary for the onset of LRI with changes in advection rate and would allow calculation of the probability of LRI given a particular advection rate.

A drawback of the work presented here is the limited amount of data available to test the model. Few experiments measure viral titer in the URT and LRT separately, but viral titer time courses alone are insufficient to allow for identifiability of all parameters of even a basic viral dynamics model (Miao et al. 2011). Our parameter correlation plots (supplementary material) indicate that even with the limiting assumption that infection parameters are the same in the two compartments, parameter correlations exist that hamper our ability to uniquely identify all parameters. Additional data that would enhance our ability to uniquely identify parameters are cell measurements in the URT and LRT. While difficult, spatially resolved infected cell time courses have been measured in mice (Manicassamy et al. 2010; Ueki et al. 2018; Fukuyama et al. 2015) and could help produce more reliable parameter estimates.

Our model is limited in other ways. While we have the flexibility to include different virus-host interactions in the LRT and URT by assuming different model parameter values for the two compartments, the results presented here have all assumed that virus-host interactions are the same in the two compartments. This was done to explicitly isolate the effect of the two transport mechanisms, but was also necessitated by the limited experimental data. In reality, differences in virus-cell interactions have been observed between cells taken from the URT and those taken from the LRT (Guo-Parke et al. 2013; Spann et al. 2014). Additionally, distributions of different cell types are known to vary as we move from the URT to the LRT (Crystal and West 1991), which means that the number of available target cells as well as the average distance between target cells changes along the respiratory tract. This will also likely alter infection dynamics along the respiratory tract. As mentioned in the methods section, our model also does not describe transitions from the eclipse phase to the infectious phase and from the infectious phase to the dead phase in the most realistic manner (Kakizoe et al. 2015; Holder and Beauchemin 2011; Beauchemin et al. 2017). While changes in the distribution for the eclipse phase can have a large impact on predicted curves for single cycle infections, the effect on multiple cycle infections, such as those shown here, is not as drastic (Holder and Beauchemin 2011). Changes in the distribution of the infectious phase alter the time course of the decay phase of multiple cycle infections and predictions about the efficacy of antiviral treatment (Beauchemin et al. 2017).

Finally, our model does not explicitly include an immune response. Many models have been proposed, at least for influenza, that contain various elements of the innate (primarily interferon) response and adaptive (Cytotoxic T lymphocytes and antibodies) response (Yan et al. 2017; Cao and McCaw 2017; Handel et al. 2018; Dobrovolny et al. 2013). While some of the effect of the immune response is implicitly contained in parameter estimates, inclusion of an explicit immune response in the model would allow comparison of reduced immune response and reduced advection as mechanisms causing LRI. We chose a simple viral model without an explicit immune response

largely because we were trying to keep the number of free parameters to a minimum. Since there are known differences in the immune response between LRT and URT (Everard et al. 1994; Plotnicky-Gilquin et al. 2000; Sealy et al. 2017), addition of an explicit immune response might require assumption of different immune response parameter values in the URT and LRT. The data sets considered in this paper do not include measurements of immune responses, making it difficult to estimate these parameters. We expect that differences in the immune response between LRT and URT will alter the prediction of this model that changes in advection are the primary drivers of LRI. An additional concern is that target cell limited models such as the one used here have difficulty accurately predicting changes in viral load caused by changes in initial viral inoculum (Li and Handel 2014; Hagensaaers et al. 1976). Changes in initial viral inoculum can also alter the strength of the immune response (Handel et al. 2018), further compounding our ability to tease out the role of different virus-host interactions in causing LRI. In addition to changing viral dynamics within a compartment (Dobrovolny et al. 2013), models with an immune response alter predictions of antiviral treatment outcomes (Cao and McCaw 2017). Should we need to investigate antiviral treatment strategies for LRT infections, a more detailed model that includes the immune response and more realistic distributions for cell transitions will be needed. In order for an expanded model to be useful, however, more data on the immune response, as well as viral and cell dynamics, in both the URT and LRT will be needed for proper parameterization.

Despite these shortcomings, this model allows for examination of the roles of diffusion and advection in preventing or allowing LRI and provides a basis for further study of spatiotemporal viral dynamics.

**Acknowledgements** The authors would like to acknowledge the assistance and helpful advice provided by Gabriela Ispas, Filip De Ridder, Dymphy Huntjens, and Dirk Roymans. Hana M. Dobrovolny received funding from Janssen R&D Belgium, and Gilberto Gonzalez-Parra's salary was paid by a grant from Janssen R&D Belgium. Pediatric patient data was provided by Janssen R&D Belgium.

## References

- Allen LJ, Schwartz EJ (2015) Free-virus and cell-to-cell transmission in models of equine infectious anemia virus infection. *Math Biosci* 270(B):237–248. <https://doi.org/10.1016/j.mbs.2015.04.001>
- Anekal SG, Zhu Y, Graham MD, Yin J (2009) Dynamics of virus spread in the presence of fluid flow. *Integr Biol* 1(11–12):664–671. <https://doi.org/10.1039/b908197f>
- Atwell JE, Geoghegan S, Karron RA, Polack FP (2016) Clinical predictors of critical lower respiratory tract illness due to respiratory syncytial virus in infants and children: data to inform case definitions for efficacy trials. *J Infect Dis* 214(11):1712–1716. <https://doi.org/10.1093/infdis/jiw447>
- Baccam P, Beauchemin C, Macken CA, Hayden FG, Perelson AS (2006) Kinetics of influenza A virus infection in humans. *J Virol* 80(15):7590–7599. <https://doi.org/10.1128/JVI.01623-05>
- Backman K, Piippo-Savolainen E, Ollikainen H, Koskela H, Korppi M (2014) Adults face increased asthma risk after infant RSV bronchiolitis and reduced respiratory health-related quality of life after RSV pneumonia. *Acta Paediatr* 103(8):850–855. <https://doi.org/10.1111/apa.12662>
- Bagga B, Woods CW, Veldman TH, Gilbert A, Mann A, Balaratnam G, Lambkin-Williams R, Oxford JS, McClain MT, Wilkinson T, Nicholson BP, Ginsburg GS, DeVincenzo JP (2013) Comparing influenza and RSV viral disease dynamics in experimentally infected adults predicts clinical effectiveness of RSV antivirals. *Antivir Ther* 18:785–791. <https://doi.org/10.3851/IMP2629>

- Bai F, Allen LJ (2019) Probability of a major infection in a stochastic within-host model with multiple stages. *Appl Math Lett* 87:1–6. <https://doi.org/10.1016/j.aml.2018.07.022>
- Beauchemin C, Samuel J, Tuszyński J (2005) A simple cellular automaton model for influenza A viral infections. *J Theor Biol* 232(2):223–234. <https://doi.org/10.1016/j.jtbi.2004.08.001>
- Beauchemin CA, Miura T, Iwami S (2017) Duration of SHIV production by infected cells is not exponentially distributed: implications for estimates of infection parameters and antiviral efficacy. *Sci Rep* 7:42765. <https://doi.org/10.1038/srep42765>
- Bocharov G, Meyerhans A, Bessonov N, Trofimchuk S, Volpert V (2016) Spatiotemporal dynamics of virus infection spreading in tissues. *PLoS ONE* 11(12):e0168576. <https://doi.org/10.1371/journal.pone.0168576>
- Bont L, Steijn M, van Aalderen W, Kimpen J (2004) Impact of wheezing after respiratory syncytial virus infection on health-related quality of life. *Pediatr Infect Dis J* 23(5):414–417. <https://doi.org/10.1097/01.inf.0000122604.32137.29>
- Branche AR, Falsey AR (2015) Respiratory syncytial virus infection in older adults: an under-recognized problem. *Drugs Aging* 32(4):261–269. <https://doi.org/10.1007/s40266-015-0258-9>
- Cao P, McCaw JM (2017) The mechanisms for within-host influenza virus control affect model-based assessment and prediction of antiviral treatment. *Viruses* 9(8):197. <https://doi.org/10.3390/v9080197>
- Crystal RG, West JB (1991) *The lung: scientific foundations*. Raven Press Ltd., New York
- Cush R, Russo P, Kucukyavuz Z, Bu Z, Neau D, Shih D, Kucukyavuz S, Ricks H (1997) Rotational and translational diffusion of a rodlike virus in random coil polymer solutions. *Macromolecules* 30(17):4920–4926. <https://doi.org/10.1021/ma970032f>
- de Oliveira-Maul JP, de Carvalho HB, Goto DM, Maia RM, Flo C, Barnabe V, Franco DR, Benabou S, Perracini MR, Jacob-Filho W, Saldiva PHN, Lorenzi-Filho G, Rubin BK, Nakagawa NK (2013) Aging, diabetes, and hypertension are associated with decreased nasal mucociliary clearance. *Chest* 143(4):1091–1097. <https://doi.org/10.1378/chest.12-1183>
- Dobrovolsky HM, Reddy MB, Kamal MA, Rayner CR, Beauchemin CA (2013) Assessing mathematical models of influenza infections using features of the immune response. *PLoS ONE* 8(2):e57088. <https://doi.org/10.1371/journal.pone.0057088>
- dos Santos R, Coutinho S (2001) Dynamics of HIV infection: a cellular automata approach. *Phys Rev Lett* 87(16):168102. <https://doi.org/10.1103/PhysRevLett.87.168102>
- Ebbert J, Limper A (2005) Respiratory syncytial virus pneumonitis in immunocompromised adults: clinical features and outcome. *Respiration* 72(3):263–269. <https://doi.org/10.1159/000085367>
- Everard M, Swarbrick A, Wrightman M, McIntyre J, Dunkley C, James P, Sewell H, Milner A (1994) Analysis of cells obtained by bronchial lavage of infants with respiratory syncytial virus infection. *Arch Dis Child* 71(5):428–432
- Fauroux B, Simoes EA, Checchia PA, Paes B, Figueras-Aloy J, Manzoni P, Bont L, Carbonell-Estrany X (2017) The burden and long-term respiratory morbidity associated with respiratory syncytial virus infection in early childhood. *Infect Dis Ther* 6(2):173–197. <https://doi.org/10.1007/s40121-017-0151-4>
- Fleming DM, Taylor RJ, Lustig RL, Schuck-Paim C, Haguinet F, Webb DJ, Logie J, Matias G, Taylor S (2015) Modelling estimates of the burden of respiratory syncytial virus infection in adults and the elderly in the united kingdom. *BMC Infect Dis* 15:443. <https://doi.org/10.1186/s12879-015-1218-z>
- Forster J, Ihorst G, Rieger C, Stephan V, Frank H, Gurth H, Berner R, Rohwedder A, Werchau H, Schumacher M, Tsai T, Petersen G (2004) Prospective population-based study of viral lower respiratory tract infections in children under 3 years of age (the PRI.DE study). *Eur J Pediatr* 163(12):709–716. <https://doi.org/10.1007/s00431-004-1523-9>
- Frank S (2000) Within-host spatial dynamics of viruses and defective interfering particles. *J Theor Biol* 206(2):279–290. <https://doi.org/10.1006/jtbi.2000.2120>
- Fukuyama S, Katsura H, Zhao D, Ozawa M, Ando T, Shoemaker JE, Ishikawa I, Yamada S, Neumann G, Watanabe S, Kitano H, Kawaoka Y (2015) Multi-spectral fluorescent reporter influenza viruses (Colorflu) as powerful tools for in vivo studies. *Nat Commun* 8:6600. <https://doi.org/10.1038/ncomms7600>
- Gallagher ME, Brooke CB, Ke R, Koelle K (2018) Causes and consequences of spatial within-host viral spread. *Viruses* 10(11):627. <https://doi.org/10.3390/v10110627>
- GBD 2015 Eastern Mediterranean Region LRI Collaborators (2017) Intravenous ribavirin for respiratory syncytial viral infections in pediatric hematopoietic SCT recipients. *Int J Publ Health*. <https://doi.org/10.1007/s00038-017-1007-0>

- Geoghegan S, Erviti A, Caballero MT, Vallone F, Zanone SM, Ves Losada J, Bianchi A, Acosta PL, Talarico LB, Ferretti A, Alva Grimaldi L, Sancilio A, Duenas K, Sastre G, Rodriguez A, Ferrero F, Barboza E, Gago GF, Nocito C, Flamenco E, Perez AR, Rebec B, Ferolla FM, Libster R, Karron RA, Bergel E, Polack FP (2017) Mortality due to respiratory syncytial virus burden and risk factors. *Am J Respir Crit Care Med* 195(1):96–103. <https://doi.org/10.1164/rccm.201603-0658OC>
- González-Parra G, Dobrovolny HM (2015) Assessing uncertainty in A2 respiratory syncytial virus viral dynamics. *Comput Math Methods Med* 2015:567589. <https://doi.org/10.1155/2015/567589>
- González-Parra G, Dobrovolny HM (2018a) Modeling of fusion inhibitor treatment of RSV in African green monkeys. *J Theor Biol* 456:62–73. <https://doi.org/10.1016/j.jtbi.2018.07.029>
- González-Parra G, Dobrovolny HM (2018b) A quantitative assessment of dynamical differences of RSV infections in vitro and in vivo. *Virology*. <https://doi.org/10.1016/j.virol.2018.07.027>
- Goodman J, Weare J (2010) Ensemble samplers with affine invariance. *Commun Appl Math Comput Sci* 5(1):65–80
- Goyal A, Murray JM (2016) Modelling the impact of cell-to-cell transmission in hepatitis B virus. *PLoS ONE* 11(8):e0161978. <https://doi.org/10.1371/journal.pone.0161978>
- Grievies JL, Yin Z, Durbin RK, Durbin JE (2015) Acute and chronic airway disease after human respiratory syncytial virus infection in cotton rats (*sigmodon hispidus*). *Comput Med* 65(4):315–326
- Grubb BR, Livraghi-Butrico A, Rogers TD, Yin W, Button B, Ostrowski LE (2016) Prophylactic administration of respiratory syncytial virus immune globulin to high-risk infants and young children. *Am J Physiol* 310(9):L860–L867. <https://doi.org/10.1152/ajplung.00015.2016>
- Guerrero-Plata A, Kolli D, Hong C, Casola A, Garofalo RP (2009) Subversion of pulmonary dendritic cell function by paramyxovirus infections. *J Immunol* 182(5):3072–3083. <https://doi.org/10.4049/jimmunol.0802262>
- Guo-Parke H, Canning P, Douglas I, Villenave R, Heaney LG, Coyle PV, Lyons JD, Shields MD, Power UF (2013) Relative respiratory syncytial virus cytopathogenesis in upper and lower respiratory tract epithelium. *Am J Respir Crit Care Med* 188(7):842–851. <https://doi.org/10.1164/rccm.201304-0750OC>
- Hagenaars T, Fischer E, Jansen C, Rebel J, Spekreijse D, Vervelde L, Backer J, de Jong M, Koets A (1976) Respiratory syncytial virus-infections in infants—quantitation and duration of shedding. *J Pediatr* 89(1):11–15. [https://doi.org/10.1016/S0022-3476\(76\)80918-3](https://doi.org/10.1016/S0022-3476(76)80918-3)
- Hall C, Long C, Schnabel K (2001) Respiratory syncytial virus infections in previously healthy working adults. *Clin Inf Dis* 33(6):792–796. <https://doi.org/10.1086/322657>
- Handel A, Li Y, McKay B, Pawelek KA, Zarnitsyna V, Antia R (2018) Exploring the impact of inoculum dose on host immunity and morbidity to inform model-based vaccine design. *PLoS Comput Biol* 14(10):e1006505. <https://doi.org/10.1371/journal.pcbi.1006505>
- Ho J, Chan K, Hu W, Lam W, Zheng L, Tipoe G, Sun J, Leung R, Tsang K (2001) The effect of aging on nasal mucociliary clearance, beat frequency, and ultrastructure of respiratory cilia. *Am J Respir Crit Care Med* 163(4):983–988
- Holder BP, Beauchemin CA (2011) Exploring the effect of biological delays in kinetic models of influenza within a host or cell culture. *BMC Public Health* 11(S1):S10. <https://doi.org/10.1186/1471-2458-11-S1-S10>
- Holder BP, Liao LE, Simon P, Boivin G, Beauchemin CAA (2011a) Design considerations in building in silico equivalents of common experimental influenza virus assays and the benefits of such an approach. *Autoimmunity*. <https://doi.org/10.3109/08916934.2011.523267>
- Holder BP, Simon P, Liao LE, Abed Y, Bouhy X, Beauchemin CA, Boivin G (2011b) Assessing the in vitro fitness of an oseltamivir-resistant seasonal A/H1N1 influenza strain using a mathematical model. *PLOS ONE* 6(3):e14767. <https://doi.org/10.1371/journal.pone.0014767>
- Hosakote YM, Brasier AR, Casola A, Garofalo RP, Kurosky A (2016) Respiratory syncytial virus infection triggers epithelial HMGB1 release as a damage-associated molecular pattern promoting a monocytic inflammatory response. *J Virol* 90(21):9618–9631. <https://doi.org/10.1128/JVI.01279-16>
- Kakizoe Y, Nakaoka S, Beauchemin CAA, Morita S, Mori H, Igarashi T, Aihara K, Miura T, Iwami S (2015) A method to determine the duration of the eclipse phase for in vitro infection with a highly pathogenic SHIV strain. *Sci Rep* 5:10371. <https://doi.org/10.1038/srep10371>
- Kaneko M, Watanabe J, Ueno E, Hida M, Sone T (2001) Risk factors for severe respiratory syncytial virus-associated lower respiratory tract infection in children. *Pediatr Int* 43(5):489–492. <https://doi.org/10.1046/j.1442-200X.2001.01438.x>



- Kesimer M, Ehre C, Burns K, Davis C, Sheehan J, Pickles R (2013) Molecular organization of the mucins and glycocalyx underlying mucus transport over mucosal surfaces of the airways. *Mucosal Immunol* 6(2):379–392. <https://doi.org/10.1038/mi.2012.81>
- Kim MC, Kim MY, Lee HJ, Lee SO, Choi SH, Kim YS, Woo JH, Kim SH (2016) CT findings in viral lower respiratory tract infections caused by parainfluenza virus, influenza virus and respiratory syncytial virus. *Medicine* 95(26):e4003. <https://doi.org/10.1097/MD.0000000000004003>
- Kusel MM, de Klerk NH, Holt PG, Kebadze T, Johnston SL, Sly PD (2006) Role of respiratory viruses in acute upper and lower respiratory tract illness in the first year of life—a birth cohort study. *Pediatr Infect Dis J* 25(8):680–686. <https://doi.org/10.1097/01.inf.0000226912.88900.a3>
- Laham F, Israele V, Casellas J, Garcia A, Prugent C, Hoffman S, Hauer D, Thumar B, Name M, Pascual A, Taratutto N, Ishida M, Balduzzi M, Maccarone M, Jackli S, Passarino R, Gaivironsky R, Karron R, Polack N, Polack F (2004) Differential production of inflammatory cytokines in primary infection with human metapneumovirus and with other common respiratory viruses of infancy. *J Infect Dis* 189(11):2047–2056. <https://doi.org/10.1086/383350>
- Lee FEH, Walsh EE, Falsey AR, Betts RF, Treanor JJ (2004) Experimental infection of humans with A2 respiratory syncytial virus. *Antivir Res* 63:191–196. <https://doi.org/10.1016/j.antiviral.2004.04.005>
- Lee N, Chan MC, Lui GC, Li R, Wong RY, Yung IM, Cheung CS, Chan EC, Hui DS, Chan PK (2015) High viral load and respiratory failure in adults hospitalized for respiratory syncytial virus infections. *J Infect Dis* 212(8):1237–1240. <https://doi.org/10.1093/infdis/jiv248>
- Li Y, Handel A (2014) Modeling inoculum dose dependent patterns of acute virus infections. *J Theor Biol* 347:63–73. <https://doi.org/10.1016/j.jtbi.2014.01.008>
- Manicassamy B, Manicassamy S, Belicha-Villanueva A, Pisanelli G, Pulendran B, Garca-Sastre A (2010) Analysis of in vivo dynamics of influenza virus infection in mice using a GFP reporter virus. *Proc Natl Acad Sci USA* 107(25):11531–11536. <https://doi.org/10.1073/pnas.0914994107>
- Mejias A, Chavez-Bueno S, Gomez AM, Somers C, Estripeaut D, Torres JP, Jafri HS, Ramilo O (2008) Respiratory syncytial virus persistence—evidence in the mouse model. *Pediatr Infect Dis J* 27(10):S60–S62. <https://doi.org/10.1097/INF.0b013e3181684d52>
- Miao H, Xia X, Perelson AS, Wu H (2011) On identifiability of nonlinear ODE models and applications in viral dynamics. *SIAM Rev* 53(1):3–39. <https://doi.org/10.1137/090757009>
- Mills J, Vankirk J, Wright P, Chanock R (1971) Experimental respiratory syncytial virus infection of adults—possible mechanisms of resistance to infection and illness. *J Immunol* 107(1):123–130
- Moore ML, Stokes KL, Hartert TV (2013) The impact of viral genotype on pathogenesis and disease severity: respiratory syncytial virus and human rhinoviruses. *Curr Opin Immunol* 25(6):761–768. <https://doi.org/10.1016/j.coi.2013.09.016>
- Murphy S, Florman A (1983) Lung defenses against infection—a clinical correlation. *Pediatrics* 72(1):1–15
- Nair H, Nokes DJ, Gessner BD, Dherani M, Madhi SA, Singleton RJ, O'Brien KL, Roca A, Wright PF, Bruce N, Chandran A, Theodoratou E, Sutanto A, Sedyaningsih ER, Ngama M, Munywoki PK, Kartasmita C, Simoes EA, Rudan I, Weber MW, Campbell H (2010) Global burden of acute lower respiratory infections due to respiratory syncytial virus in young children: a systematic review and meta-analysis. *Lancet* 375(9725):1545–1555. [https://doi.org/10.1016/S0140-6736\(10\)60206-1](https://doi.org/10.1016/S0140-6736(10)60206-1)
- Naorat S, Chittaganpitch M, Thamthitawat S, Henchaichon S, Sawatwong P, Srisaengchai P, Lu Y, Chuananon S, Amornintapichet T, Chantra S, Erdman DD, Maloney SA, Akarasewi P, Baggett HC (2013) Hospitalizations for acute lower respiratory tract infection due to respiratory syncytial virus in thailand, 2008–2011. *J Infect Dis* 203(S3):S238–S245. <https://doi.org/10.1093/infdis/jit456>
- Palmer L, Hall CB, Katkin JP, Shi N, Mazaquel AS, McLaurin KK, Mahadevia PJ (2010) Healthcare costs within a year of respiratory syncytial virus among medicaid infants. *Pediatr Pulmonol* 45(8):772–781. <https://doi.org/10.1002/ppul.21244>
- Park SY, Kim T, Jang YR, Kim MC, Chong YP, Lee SO, Choi SH, Kim YS, Woo JH, Kim SH (2017) Factors predicting life-threatening infections with respiratory syncytial virus in adult patients. *Infect Dis* 49(5):333–340. <https://doi.org/10.1080/23744235.2016.1260769>
- Parkinson D, Mukherjee P, Liddle AR (2006) Bayesian model selection analysis of WMAP3. *Phys Rev D* 73(12):123523. <https://doi.org/10.1103/PhysRevD.73.123523>
- Perez-Yarza EG, Moreno A, Lazaro P, Mejias A, Ramilo O (2007) The association between respiratory syncytial virus infection and the development of childhood asthma—a systematic review of the literature. *Pediatr Infect Dis J* 26(8):733–739. <https://doi.org/10.1097/INF.0b013e3180618c42>
- Piedimonte G (2013) Respiratory syncytial virus and asthma: speed-dating or long-term relationship? *Curr Opin Pediatr* 25(3):344–349. <https://doi.org/10.1097/MOP.0b013e328360bd2e>

- Plotnicky-Gilquin H, Robert A, Chevalet L, Haeuw J, Beck A, Bonnefoy J, Brandt C, Siegrist C, Nguyen T, Power U (2000) CD4(+) T-cell-mediated antiviral protection of the upper respiratory tract in BALB/c mice following parenteral immunization with a recombinant respiratory syncytial virus G protein fragment. *J Virol* 74(8):3455–3463. <https://doi.org/10.1128/JVI.74.8.3455-3463.2000>
- Poulsen A, Stensballe LG, Nielsen J, Benn CS, Balde A, Roth A, Lisse IM, Aaby P (2006) Long-term consequences of respiratory syncytial virus acute lower respiratory tract infection in early childhood in Guinea-Bissau. *Pediatr Inf Dis J* 25(11):1025–1031. <https://doi.org/10.1097/01.inf.0000243214.80794.3a>
- Prince GA, Porter DD (1976) The pathogenesis of respiratory syncytial virus infection in infant ferrets. *Am J Pathol* 82(2):339–350
- Puchelle E, Zahm J, Bertrand A (1979) Influence of age on bronchial mucociliary transport. *Scand J Respir Dis* 60(6):307–313
- Reperant LA, Kuiken T, Grenfell BT, Osterhaus ADME, Dobson AP (2012) Linking influenza virus tissue tropism to population-level reproductive fitness. *PLoS ONE* 7(8):e43115. <https://doi.org/10.1371/journal.pone.0043115>
- Robert D, Verbiest D, Demey H, Ieven M, Jansens H, Jorens P (2008) A series of five adult cases of respiratory syncytial virus-related acute respiratory distress syndrome. *Anaesth Intensive Care* 36(2):230–234
- Ruckwardt TJ, Morabito KM, Graham BS (2016) Determinants of early life immune responses to RSV infection. *Curr Opin Virol* 16:151–157. <https://doi.org/10.1016/j.coviro.2016.01.003>
- Sealy RE, Surman SL, Hurwitz JL (2017) CD4(+) T cells support establishment of RSV-specific IgG and IgA antibody secreting cells in the upper and lower murine respiratory tract following RSV infection. *Vaccine* 35(20):2617–2621. <https://doi.org/10.1016/j.vaccine.2017.03.073>
- Shi T, Balsells E, Wastnedge E, Singleton R, Rasmussen Z, Zar HJ, Rath BA, Madhi SA, Campbell S, Vaccari LC, Bulkow LR, Thomas ED, Barnett W, Hoppe C, Campbell H, Nair H (2015) Risk factors for respiratory syncytial virus associated with acute lower respiratory infection in children under five years: systematic review and meta-analysis. *J Global Health* 5(2):203–215. <https://doi.org/10.7189/jogh.05.020416>
- Spann KM, Baturcam E, Schagen J, Jones C, Straub CP, Preston FM, Chen L, Phipps S, Sly PD, Fantino E (2014) Viral and host factors determine innate immune responses in airway epithelial cells from children with wheeze and atopy. *Thorax* 69(10):918–925. <https://doi.org/10.1136/thoraxjnl-2013-204908>
- Stoffer D, Wall K (1991) Bootstrapping state-space models: Gaussian maximum likelihood estimation and the kalman filter. *J Am Stat Assoc* 86(416):1024–1033. <https://doi.org/10.2307/2290521>
- Strain M, Richman D, Wong J, Levine H (2002) Spatiotemporal dynamics of HIV propagation. *J Theor Biol* 218(1):85–96. <https://doi.org/10.1006/jtbi.3055>
- Sturm R (2012) Theoretical models of carcinogenic particle deposition and clearance in children's lungs. *J Thorac Dis* 4(4):368–376. <https://doi.org/10.3978/j.issn.2072-1439.2012.08.03>
- Takeyama A, Hashimoto K, Sato M, Kawashima R, Kawasaki Y, Hosoya M (2016) Respiratory syncytial virus shedding by children hospitalized with lower respiratory tract infection. *J Med Virol* 88(6):938–946. <https://doi.org/10.1002/jmv.24434>
- Tregoning JS, Schwarze J (2010) Respiratory viral infections in infants: causes, clinical symptoms, virology, and immunology. *Clin Microbiol Rev* 23(1):74–98. <https://doi.org/10.1128/CMR.00032-09>
- Ueki H, Wang IH, Fukuyama S, Katsura H, da Silva Lopes TJ, Neumann G, Kawaoka Y (2018) In vivo imaging of the pathophysiological changes and neutrophil dynamics in influenza virus-infected mouse lungs. *Proc Natl Acad Sci USA* 115(18):E6622–E6629. <https://doi.org/10.1073/pnas.1806265115>
- Vareille M, Kieninger E, Edwards MR, Regamey N (2011) The airway epithelium: soldier in the fight against respiratory viruses. *Clin Microbiol Rev* 24(1):210–229. <https://doi.org/10.1128/CMR.00014-10>
- Walpita P, Johns LM, Tandon R, Moore ML (2015) Mammalian cell-derived respiratory syncytial virus-like particles protect the lower as well as the upper respiratory tract. *PLoS ONE* 10(7):e0130755. <https://doi.org/10.1371/journal.pone.0130755>
- Walsh EE, Peterson DR, Falsey AR (2013) Viral shedding and immune responses to respiratory syncytial virus infection in older adults. *J Infect Dis* 207:1424–1432. <https://doi.org/10.1093/infdis/jit038>
- Wang X, Tang S, Song X, Rong L (2017) Mathematical analysis of an HIV latent infection model including both virus-to-cell infection and cell-to-cell transmission. *J Biol Dyn* 11(2):455–483. <https://doi.org/10.1080/17513758.2016.1242784>

- Wolf D, Greenberg D, Kalkstein D, Shemer-Avni Y, Givon-Lavi N, Saleh N, Goldberg M, Dagan R (2006) Comparison of human metapneumovirus, respiratory syncytial virus and influenza A virus lower respiratory tract infections in hospitalized young children. *Pediatr Inf Dis J* 25(4):320–324. <https://doi.org/10.1097/01.inf.0000207395.80657.cf>
- Worden K, Hensman J (2012) Parameter estimation and model selection for a class of hysteretic systems using bayesian inference. *Mech Syst Signal Process* 32:153–169
- Yan AW, Cao P, Mccaw JM (2016) On the extinction probability in models of within-host infection: the role of latency and immunity. *J Math Biol* 73(4):787–813. <https://doi.org/10.1007/s00285-015-0961-5>
- Yan AW, Cao P, Heffernan JM, McVernon J, Quinn KM, La Gruta NL, Laurie KL, Mccaw JM (2017) Modelling cross-reactivity and memory in the cellular adaptive immune response to influenza infection in the host. *J Theor Biol* 413:34–49. <https://doi.org/10.1016/j.jtbi.2016.11.008>
- Zeng R, Li C, Li N, Wei L, Cui Y (2011) The role of cytokines and chemokines in severe respiratory syncytial virus infection and subsequent asthma. *Cytokine* 53(1):1–7. <https://doi.org/10.1016/j.cyto.2010.09.011>
- Zhao Y, Jamaluddin M, Zhang Y, Sun H, Ivanciuc T, Garofalo RP, Brasier AR (2017) Systematic analysis of cell-type differences in the epithelial secretome reveals insights into the pathogenesis of respiratory syncytial virus-induced lower respiratory tract infections. *J Immunol* 198(8):3345–3364. <https://doi.org/10.4049/jimmunol.1601291>

**Publisher's Note** Springer Nature remains neutral with regard to jurisdictional claims in published maps and institutional affiliations.